

---

# Experimental study of convective heat transfer in $\text{Fe}_3\text{O}_4 - \text{H}_2\text{O}$ nanofluids in a grid-shaped microchannel under magnetic field

Chunquan LI<sup>a</sup>, Zhengwei LIU<sup>a</sup>, Hongyan HUANG<sup>a</sup>, Yuling SHANG<sup>b,\*</sup>, Xuebin LI<sup>a</sup>

<sup>a</sup> School of Mechanical and Electrical Engineering, Guilin University of Electronic Technology, Guilin, China

<sup>b</sup> School of Electronic Engineering and Automation, Guilin University of Electronic Technology, Guilin, China

\* Corresponding author: E-mail : syl@guet.edu.cn

*Abstract: Experimental study of convective heat transfer with  $\text{Fe}_3\text{O}_4 - \text{H}_2\text{O}$  (1 vol%) nanofluids was examined when the nanofluids flowed through a gridded microchannel under a perpendicularly oriented magnetic field of 0-700 G strength. The results show that, compared to deionized water, nanofluids reduces chip temperature by 2.11 °C and increases the convective heat transfer coefficient by 30.43 % when no magnetic field is present. Under magnetic field conditions, the chip temperature was maximally reduced by 3.2 °C, while the convective heat transfer coefficient is improved up to 65 % in comparison to deionized water. With increasing magnetic field strength, nanofluids's pressure drop and flow resistance showed an overall decreasing trend, and the pressure drop at 500 G and 700 G were reduced by 19.3 % and 14.51 %, respectively, compared to that at 0 G. In terms of overall performance, improved heat transfer in the presence of a magnetic field outperforms heat transfer in the absence of a magnetic field. The intensive heat transfer factor of nanofluids under magnetic field conditions is greater than one when the Reynolds number exceeds 400. The best overall performance and the highest intensive heat transfer factor are observed at a magnetic field strength of 300 G.*

*Keywords: Magnetic nanofluids; Gridded microchannel; Magnetic field; Intensive heat transfer*

## 1. Introduction

Today, electronic devices tend to be tiny, with high-density, and complex due to the rapid development of the electronics industry [1]. The problem of heat failure in electronic devices is becoming ever more serious [2]. Therefore, a new method of heat dissipation needs to be found for microelectronic heat dissipation [3] [4]. Microchannels can be used as a new type of heat exchanger due to their high-density structure and strong convective heat transfer characteristics [5, 6]. Nanofluids have higher thermal conductivity compared to deionized water and ethylene glycol, can be used as new coolants [7][8]. The use of  $\text{Al}_2\text{O}_3 - \text{H}_2\text{O}$  nanofluids in microchannels improves heat transfer performance, according to Seyf [9], Mital [10], and Sakanova [11], and the concentration of nanoparticles has a substantial influence on the flow heat dissipation properties of microchannels. Sundar et al. [12] conducted experiments with a volume fraction of 0.6 % nanofluids in a turbulent state and found that as the friction coefficient increased by 10.01 %, the thermal conductivity also increased by 30.96 %. Sakanova [13] used  $\text{Al}_2\text{O}_3 - \text{H}_2\text{O}$  nanofluids as the heat transfer medium in copper-based microchannels and found that nanofluids (5 vol%) improved cooling performance by 17.3 %. The experiments by Li [14] show that in the serpentine microfluidic channel, the

$\text{Al}_2\text{O}_3 - \text{H}_2\text{O}$  nanofluids makes the flow resistance and heat transfer coefficient increase compared to water, but in a comprehensive analysis, nanofluids has a stronger heat transfer effect than deionized water. Ghofrani et al. [15] investigated magnetic fluid viscosity under magnetic field excitation and discovered that the magnetic field increases magnetic fluid viscosity. According to Goharkhah et al. [16], a magnetic field can improve magnetic fluid heat transfer performance, as well as a distinct Reynolds number corresponding to appropriate magnetic field strength, and that magnetism rises as the Reynolds number increases. Sha et.al. [17] experimental studies have shown that the concentration, temperature and magnetic field size of the magnetic nanofluids have an effect on the heat transfer performance of the nanofluids. When a 4.7 vol % magnetic fluid was subjected to a 0.1 T transverse magnetism, Parekh and Lee [18] found that the greatest thermal conductivity enhancement was 30 %.

In conclusion, the investigation of flow heat transfer characteristics using a combination of applied magnetic field excitation, microchannels as heat dissipation channels, and magnetic nanofluids as a heat transfer medium will become a hot topic for domestic and worldwide research.

## 2. Experimental methods

### 2.1. Experimental system

The diagram and the photograph of the experimental setup are shown on Fig. 1 and Fig. 2, respectively. The experimental platform is composed of a heat source, circulating flow system, magnetic field generator, and data acquisition system. The heat source and magnetic field generator consist of a high-temperature ceramic sheet, electromagnet, and regulated DC power supply. We are changing the heat flow density and magnetic field strength by adjusting the regulated power supply. The circulating flow system includes a microchannel, a connecting fixture, a power pump, a thermostatic water tank, and a cooling water tank. The data acquisition system comprises of a data collector (Agilent-34970A), the T-type thermocouple, and a pressure Gauge.

In Fig. 3, the microchannel cold plate is  $40 \times 40 \times 5$  mm in size and is made of HPb59-1 (easy cutting brass).

As shown in Fig. 4(a), T.P #1 is the upper surface temperature measurement point, T.P # 2 to T.P # 6 are the wall temperature measurement points, and T.P # 2 measures the lower surface of the chip and the middle position of the wall of the cold plate. Fig. 4(b), schematic diagram of magnetic field lines.

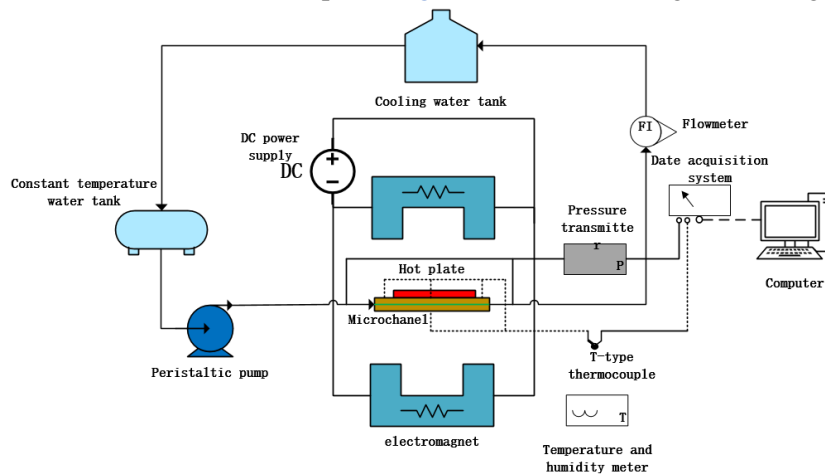
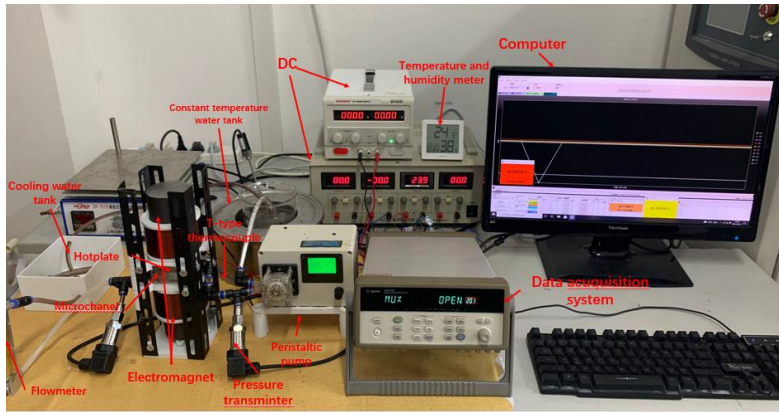
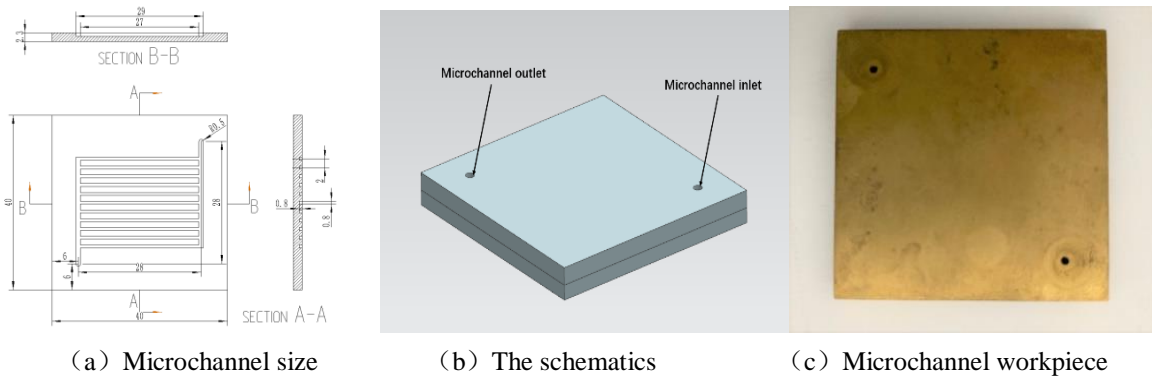


Fig. 1. The diagram of the experimental setup



**Fig. 2.** The photograph of the experimental setup

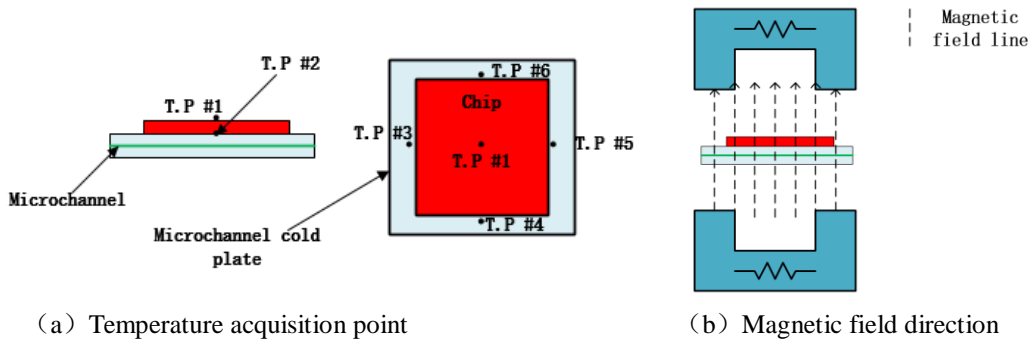


(a) Microchannel size

(b) The schematics

(c) Microchannel workpiece

**Fig. 3.** The microchannel of grid shape



(a) Temperature acquisition point

(b) Magnetic field direction

**Fig. 4.** The diagram of the experimental device

## 2.2. Nanofluids preparation

Using a two-step method, we used CTAB (Hexadecyltrimethylammonium bromide) as the dispersant and deionized water as the base solution for making the  $Fe_3O_4 - H_2O$  (1 vol%) nanofluids. A scanning electron micrograph of nanoparticles is shown in Fig. 5.

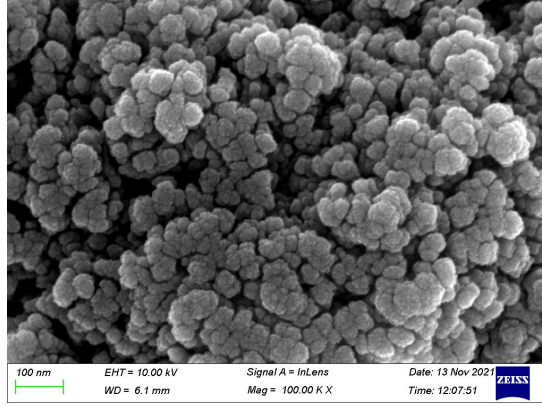


**Fig. 5.** SEM diagram of nanoparticles

### 2.3. Experimental platform verification

To test the stability of the experimental setup, the thermal equilibrium deviation was analyzed [14].

$$\varepsilon = \frac{|Q_{MCH} - Q|}{0.5(Q_{MCH} + Q)} \quad (1)$$

As shown in Fig. 6, the deviation in the balance between heat generation and heat removal by water is within 7 %, which shows that the experimental circulation system is reliable.

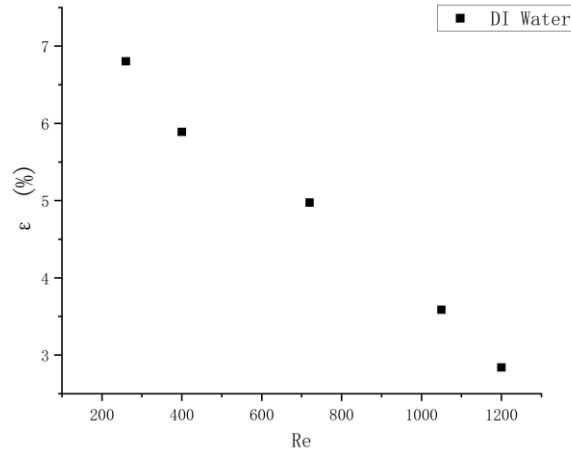


**Fig. 6.** Deviation of thermal equilibrium

## 3. Data Analysis and Uncertainty Analysis

### 3.1. Data Analysis

The equivalent diameter of gridded microchannel:

$$D_s = \frac{2W_s H_s}{W_s + H_s} \quad (2)$$

Density:

$$\rho_{nf} = (1 - \phi)\rho_p \quad (3)$$

Reynolds Number:

$$Re = \frac{\rho v D_s}{\mu} \quad (4)$$

The chip temperature is obtained by averaging the temperatures of the top and bottom surfaces of the chip:

$$T_c = \frac{(T_s - T_x)}{2} \quad (5)$$

The average temperature of the fluid is:

$$T_{nf} = \frac{1}{2} (T_i + T_o) \quad (6)$$

The wall temperature is obtained by averaging five uniformly distributed temperature measurement points:

$$T_w = \frac{1}{5} \sum_{i=1}^5 T_{wi} \quad (7)$$

Average convective heat transfer coefficient:

$$h = \frac{Q}{(T_w - T_{nf}) S_w} \quad (8)$$

Nusselt number:

$$Nu = \frac{h D_s}{k} \quad (9)$$

Flow resistance:

$$f = \frac{\Delta P \cdot D_s}{2L \rho_{nf} v^2} \quad (10)$$

Intensive heat transfer factor:

$$\eta = \frac{Nu_{nf}/Nu_f}{(f_{nf}/f_f)^{\frac{1}{3}}} \quad (11)$$

### 3.2. Uncertainty analysis

An experimental uncertainty analysis is performed as follows:

**Table 1** Uncertainty of variable factors of the experimental system.

| Variable factors    | Uncertainty |
|---------------------|-------------|
| Equivalent diameter | 6.5 %       |
| Magnetic field      | 4.5 %       |
| Heat source system  | 5 %         |
| Nusselt Number      | 9.57 %      |
| Reynolds number     | 6.52 %      |
| Flow resistance     | 6.15 %      |

## 4. Analysis of experimental results

### 4.1. Flow characteristic analysis

When the magnetic field increases, the nanofluids pressure drops and the resistance to flow decreases at the same Reynolds number, as may be seen in Fig. 7 and Fig. 8 (water temperature was

25 °C). This is because, in the absence of a magnetic field ( $B = 0$  G), the collision and agglomeration between nanoparticles will occur during the flow of nanofluids, precipitation will happen, and so the pressure drop and flow resistance will increase. Under the influence of the magnetic field, the nanoparticles can overcome the gravity under the magnetism in the vertical direction, and the nanoparticles can be stably suspended in the nanofluids, which reduces the phenomenon of nanoparticle settling. When the magnetic field is further enhanced, more nanoparticles overcome gravity and adsorb on the microchannel wall, increasing the pressure drop and the flow resistance.

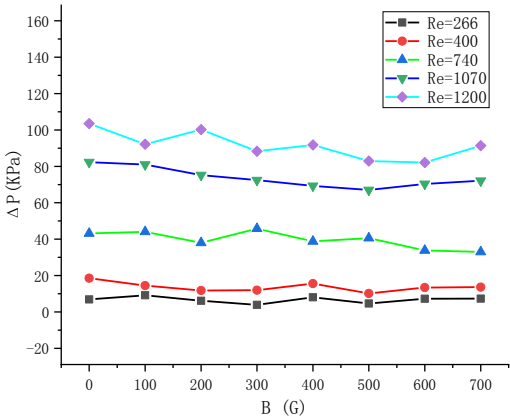


**Fig. 7.** Variation of pressure drop with the magnetic field

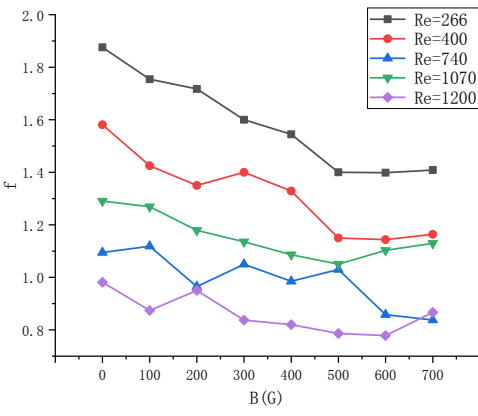


**Fig. 8.** Variation of flow resistance with the magnetic field

**4.2. Analysis of heat transfer characteristics**

In Fig. 9 it is shown that under the condition of no magnetic field ( $B = 0$  G), the nanofluids reduces the chip temperature by up to 2.11 °C, compared to deionized water. As the Reynolds number increases, the chip temperature decreases. When the magnetic field increases to 400 G, the reduction rate of chip temperature also increases, from 6.7 % at 0 G to 10.29 % at 400 G. However, when the magnetic field increases to about 700 G, the reduction rate of chip temperature decreases to about 9 %.

Nanofluids and water's convective heat transfer coefficients were compared under different magnetic field conditions and the results are shown in Fig. 10. Under the condition of no magnetic field ( $B = 0$  G), the nanofluids improves the convective heat transfer coefficient by 30.43 %. With increasing magnetic field intensity from 0 to 300 G, the augmentation rate of convective heat transfer coefficient increased, from 30.43 % at 0 G to 64.54 % at 300 G. When the magnetic field intensity is increased even further, the reduction rate of convective heat transfer coefficient decreases to about 50 %.

With a small equivalent diameter of the microchannel, the nanoparticles can overcome the Brownian motion energy due to the small magnetic field force and gather into magnetic chains in the magnetic field direction. At the same time, the nanoparticles form magnetic chains that can further increase heat transfer. As the magnetic field increases further, particle congestion tends to occur in the microchannel, and the heat carried away by the flow is reduced.

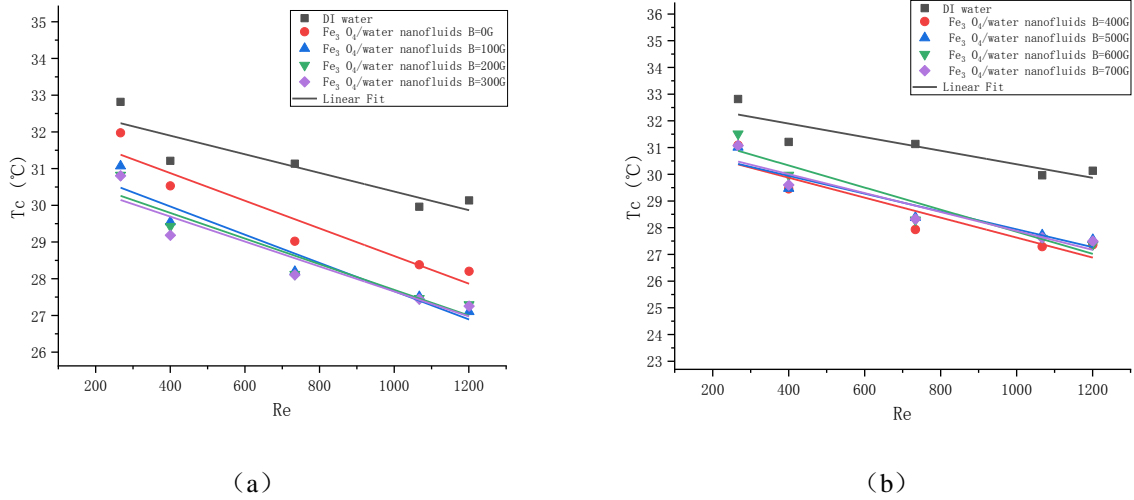


Fig. 9. Under varied magnetic field strengths, the chip temperature changes

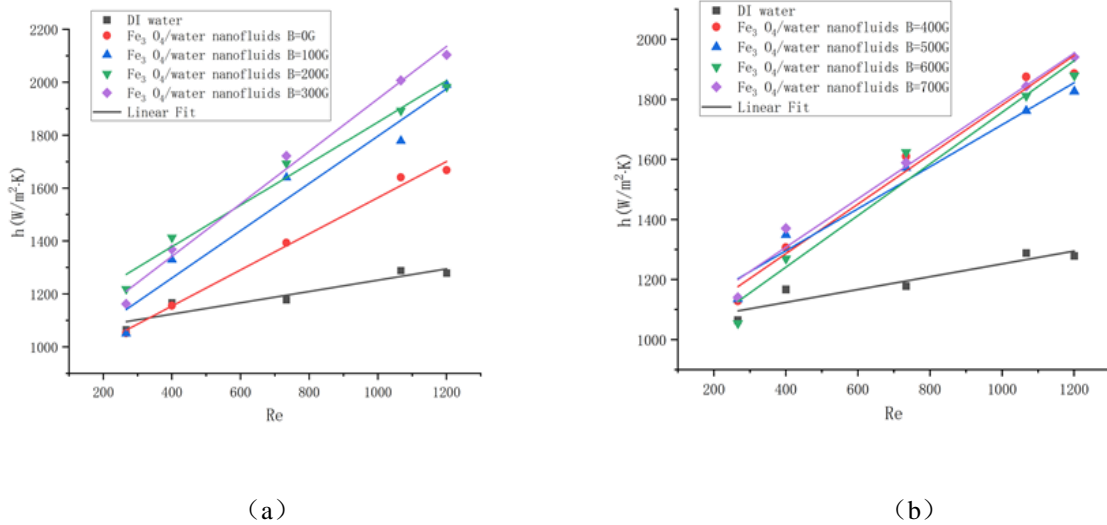
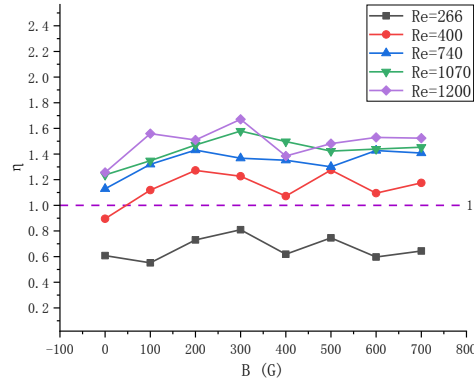


Fig. 10. Under varied magnetic field strengths, the convective heat transfer coefficient changes

### 4.3. Intensive heat transfer factor analysis

From Fig. 11 it may be seen that the intensive heat transfer factor of 1% volume fraction  $Fe_3O_4 - H_2O$  nanofluids, with Reynolds number in the range of 200 - 1200, shows an increasing trend with the increase of the magnetic field strength [14]. When the Reynolds number is 266 the intensive heat transfer factor of nanofluids under the magnetic field is less than 1. This suggests that at Reynolds number 266 the nanofluids has a worse overall performance than the deionized water. When the Reynolds number is 400, the all-around performance of nanofluids under the condition of no magnetic field ( $B = 0$  G) is worse than in the case of the deionized water. When the magnetic field strength increases to more than 100 G, the nanofluids has an intensive heat transfer factor of more than one. For the Reynolds number in the range of 740 - 1200, the magnetic nanofluids have a superior heat transfer performance than water, which shows the significant and economical enhanced heat transfer of  $Fe_3O_4 - H_2O$  nanofluids. At a magnetic field strength around 300 G, the average intense heat transfer factor was the greatest and best all-around performance is observed.



**Fig. 11.** Strengthening factor relation

## 5. Conclusions

Nanofluids with 1 % volume concentration were prepared using nanoparticles with a particle size of 20 nm on average, and nanofluids flow and heat dissipation properties in microchannels under different magnetic field strength conditions were experimentally analyzed, with Reynolds number in the range of 266 – 1200. The main conclusions are the following:

1. Compared to deionized water, nanofluids reduces chip temperature by 2.11 °C and increases convective heat transfer coefficient by 30.43% when no magnetic field is present.
2. When compared to deionized water, the magnetic fluid used in a magnetic field lowers the chip temperature up to 3.2 °C and enhances the convective heat transfer coefficient up to 65 %.
3. With increasing magnetic field strength, the nanofluids's pressure drop and flow resistance showed an overall decreasing trend, and the pressure drop at 500 G and 700 G were reduced by 19.3 % and 14.51 %, respectively, compared to that at 0 G.
4. The intensive heat transfer factor of nanofluids under magnetic field conditions is greater than one when the Reynolds number exceeds 400. When compared to deionized water, the improved heat transfer impact is very significant. The average intensive heat transfer factor at a magnetic field strength of 300 G is the largest and the best overall performance is noted.

## Nomenclature:

|            |  |                   |  |
|------------|--|-------------------|--|
| $B$        | Magnetic flux density, G                     | $f$               | Flow resistance                        |
| $h$        | Convective heat transfer coefficient         | $\Delta P$        | Differential pressure drop, Pa         |
| $k$        | Thermal conductivity, $W/m \cdot k$          | <i>Greek</i>      |  |
| $W_s, H_s$ | Microchannel interface size, mm              | $\rho$            | Density, kg/m <sup>3</sup>             |
| $D_s$      | Equivalent diameter, mm                      | $\nu$             | Fluid velocity, m/s                    |
| $T_s, T_x$ | Chip upper and lower surface temperature, °C | $\mu$             | Dynamic viscosity, $Pa \cdot s$        |
| $T_C$      | Chip temperature, °C                         | $\varphi$         | Volume percent, vol%                   |
| $T_w$      | Cold plate surface temperature, °C           | $\varepsilon$     | Thermal equilibrium deviation, %       |
| $T_i, T_o$ | Inlet and outlet temperature, °C             | $\eta$            | Intensive heat transfer factor, Eq. 11 |
| $T_{nf}$   | Average temperature of fluid, °C             | <i>Subscripts</i> |  |
| $Nu$       | Nusselt Number                               | f                 | Base fluid                             |
| $Q$        | Heat flux, W/m <sup>2</sup>                  | nf                | Fluid                                  |



## Acknowledgement:

This work is supported by the National Natural Science Foundation of China (Nos. 61661013, 51465013).

## References

- [1] Selvakumar, P., et al., Investigations of effect of radial flow impeller type swirl generator fitted in an electronic heat sink and  $\text{Al}_2\text{O}_3$ /water nanofluids on heat transfer enhancement, *Chemical Engineering and Processing Process Intensification*, 72(2013), pp.103-112
- [2] Ho, C. J., et al., Efficacy of divergent minichannels on cooling performance of heat sinks with water-based MEPCM suspensions, *International Journal of Thermal Sciences*, 130(2018), pp.333-346
- [3] Behzad, F., et al., Effect of nanoparticles size on thermal performance of nanofluids in a trapezoidal microchannel- heat-sink, *International Communications in Heat and Mass Transfer*, 45(2013), pp.155-161
- [4] Ho, C. J., et al., Comparative study on thermal performance of MEPCM suspensions in parallel and divergent minichannel heat sinks, *International Communications in Heat and Mass Transfer*, 94(2018), pp.96-105
- [5] Zhai, Y. L., et al., Heat transfer enhancement of  $\text{Al}_2\text{O}_3 - \text{H}_2\text{O}$  nano-fluids flowing through a micro heat sink with complex structure, *International Communications in Heat and Mass Transfer*, 66(2015), pp.158-166
- [6] Sohel, M. R. , et al., An experimental investigation of heat transfer enhancement of a minichannel heat sink using  $\text{Al}_2\text{O}_3 - \text{H}_2\text{O}$  nanofluids, *International Journal of Heat and Mass Transfer*, 74(2014), pp.164-172
- [7] Solangi, K. H, et al., A comprehensive review of thermo-physical properties and convective heat transfer to nanofluids, *Energy*, 89(2015), pp.1065-1086
- [8] Bhogare, R. A, and Kothawale, B. S., Performance investigation of Automobile Radiator operated with  $\text{Al}_2\text{O}_3$  based nanofluids, *IOSR Journal of Mechanical and Civil Engineering*, 11(2014), 3, pp. 23-30
- [9] Seyf, H. R, and Feizbakhshi, M., Computational analysis of nanofluids effects on convective heat transfer enhancement of micro-pin-fin heat sinks, *International Journal of Thermal Sciences*, 58(2012), pp.168-179
- [10] Mital, M., Analytical analysis of heat transfer and pumping power of laminar nanofluids developing flow in microchannels, *Applied Thermal Engineering*, 50(2013),1, pp.429-436
- [11] Sakanova, A, et al., Performance improvements of microchannel heat sink using wavy channel and nanofluids, *International Journal of Heat and Mass Transfer*, 89( 2015) pp. 59-74
- [12] Sundar, L. S., et al., Experimental investigation of forced convection heat transfer and friction factor in a tube with  $\text{Fe}_3\text{O}_4$  magnetic nanofluids, *Experimental Thermal and Fluid Science*. 37 (2012) , pp.65–71
- [13] Sakanova, A., et al., Optimization and comparison of double-layer and double-side micro-channel heat sinks with nanofluids for power electronics cooling, *Applied Thermal Engineering*, 65(2014),1-2, pp.124-134
- [14] Li, C., et al., Study on the flow and heat dissipation of water-based alumina nanofluids in microchannels, *Case Studies in Thermal Engineering*, 22(2020) pp.100746

- [15] Ghofrani, A., et al., Experimental investigation on laminar forced convection heat transfer of ferrofluids under an alternating magnetic field, *Experimental Thermal and Fluid Science*, 49(2013), pp.193-200
- [16] Goharkhah, M., et al., Convective heat transfer characteristics of magnetite nanofluids under the influence of constant and alternating magnetic field, *Powder Technology*, 274 (2015), pp. 258–267
- [17] Sha, L., et al., Experimental investigation on the convective heat transfer of  $\text{Fe}_3\text{O}_4$  /water nanofluids under constant magnetic field, *Applied Thermal Engineering*, 113(2017), pp. 566-574
- [18] Parekh, K. and Lee, H. S., Magnetic field induced enhancement in thermal conductivity of magnetite nanofluids, *Journal of Applied Physics*, 107 (2010) pp.09A310-09A310

Paper Submitted: 20.06.2022

Paper Revised: 30.08.2022

Paper Accepted: 06.09.2022